Materials Characterization 144 (2018) 66–76

Contents lists available at ScienceDirect

Materials Characterization

journal homepage: www.elsevier.com/locate/matchar

Effect of isochronal annealing on the microstructure, texture and mechanical properties of a cold-rolled high manganese steel

Sudipta Pramanik[a,*], Ahmed A. Saleh[a], Elena V. Pereloma[a,b], Azdiar A. Gazder[b]

[a] School of Mechanical, Materials, Mechatronic and Biomedical Engineering, University of Wollongong, New South Wales 2522, Australia
[b] Electron Microscopy Centre, AIIM, Innovation Campus, Squires Way, Wollongong, New South Wales 2500, Australia

ARTICLE INFO

Keywords:
High Mn steel
Phase transformation
Transformation induced plasticity
Electron back-scattering diffraction (EBSD)
Transmission electron microscopy (TEM)

ABSTRACT

A Fe-17Mn-3Al-2Si-1Ni-0.06C wt.% steel was subjected to cold-rolling to 42% thickness reduction and isochronally annealed for 300 s between 500 and 850 °C. The high Mn steel was characterised via electron back-scattering diffraction, transmission electron microscopy and uniaxial tensile testing. The reversion of deformation-induced ε and α′-martensite to austenite (γ) was witnessed with the formation of fine twins in reverted/recovered γ grains after annealing to 650 °C. The nucleation of new γ grains at the boundary of reverted/recovered γ grains was also noted. Upon reversion, the γ orientations originated from the ε and α′-martensite orientations by phase transformation via the Shoji-Nishiyama and Kurdjumov-Sachs orientation relationships, respectively. Upon segmenting the γ grains, the recrystallised γ grains were observed to nucleate with orientations similar to those of the reverted/recovered γ grains. Uniaxial tension on a fully recrystallised γ microstructure showed that the initial γ grain size has a more significant effect on the yield strength than the ε and α′-martensite fractions. On the other hand, the initial ε and α′-martensite fractions affect the total elongation.

1. Introduction

High strength steels containing 15–20 wt.% manganese possess low stacking fault energies (SFE) that enable the metastable face-centred cubic (fcc) austenite (γ) phase to accommodate deformation by a combination of perfect and partial slip, twinning and phase transformation to hexagonal closed packed (hcp) ε-martensite and/or body-centred cubic (bcc) α′-martensite [1–3]. Generally, steels with SFE less than ~21 mJ/m^2 result in the formation of ε and α′-martensite whereas SFE between ~12–21 mJ/m^2 result in the formation of twins and ε and α′-martensite. The pathways to phase transformation are: (i) γ directly transforming to α′-martensite and (ii) γ transforming to α′-martensite via prior transformation to ε-martensite [1, 4].

Upon annealing, the deformation-induced ε and α′-martensite revert to γ; with the latter phase undergoing subsequent recrystallisation [1, 3, 5–7]. The reverse transformation of ε-martensite occurs between 100 and 250 °C while the reversion of α′-martensite occurs between 500 and 700 °C for the high Mn steel used in the present investigation [8]. Lü et al. [3] reported the formation of highly dislocated, reverted γ when an Fe-21.6Mn-0.38C steel (all compositions in wt.% from here on) cold-rolled to 50% thickness reduction was subsequently annealed at 630 °C. Kowalska et al. [7] observed fine twins in reverted γ along with remnant deformation-induced α′-martensite when an Fe-26Mn-3Al-3Si steel cold-rolled to 57% thickness reduction was annealed at 500 °C. In that study, the onset of γ recrystallisation was noted at 650 °C.

Upon annealing, the orientations of reverted γ are derived from the orientations of their deformation-induced ε and α′-martensite counterparts via the Shoji-Nishiyama (S-N, $\{111\}_\gamma \parallel \{0001\}_\varepsilon$, $\langle 110\rangle_\gamma \parallel \langle 11\bar{2}0\rangle_\varepsilon$ [9]) and the Kurdjumov-Sachs (K-S, $\{111\}_\gamma \parallel \{110\}_{\alpha'}$, $\langle 110\rangle_\gamma \parallel \langle 111\rangle_{\alpha'}$ [10]) orientation relationships, respectively. In this regard, Lü et al. [3] showed the reversion of $\{01\bar{1}4\}\langle 1\bar{2}12\rangle_\varepsilon$ to $\{123\}\langle 412\rangle_\gamma$ in an Fe-21.6Mn-0.38C steel cold-rolled to 50% thickness reduction and annealed at 630 °C. Kowalska et al. [7] observed reversion to the Brass (Br_γ, $\{110\}\langle 112\rangle_\gamma$), Copper ($Cu_\gamma$, $\{112\}\langle 111\rangle_\gamma$), Goss ($G_\gamma$, $\{110\}\langle 001\rangle_\gamma$) and S_γ ($\{123\}\langle 634\rangle_\gamma$) orientations from the $\{hkil\}_\varepsilon$–fibre orientations and $\{001\}\langle 110\rangle_{\alpha'}$, $(112)[1\bar{1}0]_{\alpha'}$ when an Fe-26Mn-3Al-3Si steel cold-rolled to 57% thickness reduction was subjected to isochronal annealing at 500, 650 and 750 °C.

Annealed high Mn steels are reported to possess ultimate tensile strengths (UTS) and total elongation greater than 1100 MPa and 0.55, respectively [11, 12]. A comprehensive collection of literature-based tensile properties of metastable high Mn steels has been presented by the authors in Ref. [13]. High Mn steels processed by cold-rolling and annealing after hot-rolling and solution treatment [14, 15] show slightly higher UTS compared to steels processed by hot-rolling and solution treatment only [16–18]; primarily on account of the smaller γ

* Corresponding author.
E-mail address: sp345@uowmail.edu.au (S. Pramanik).

https://doi.org/10.1016/j.matchar.2018.06.022
Received 21 February 2018; Received in revised form 13 June 2018; Accepted 13 June 2018
Available online 18 June 2018

grain size in the former case. In addition, multi-phase high Mn steels [8] tend to possess higher yield strengths (YS) and UTS of 465–1231 MPa and 856–1376 MPa compared to their single-phase counterparts (YS = 168–434 MPa, UTS = 698–822 MPa) [14].

The Fe-17Mn-3Al-2Si-1Ni-0.06C steel of this study was cold-rolled to 66% thickness reduction and subjected to isochronal annealing. Microstructure characterisation via transmission Kikuchi diffraction (TKD) by Gazder et al. [5, 6] revealed the formation of deformation-induced ε and α′-martensite and a trace amount of γ upon cold-rolling. Upon annealing at 625 °C, the microstructure comprised a predominant fraction of reverted and recrystallised γ (with the recrystallised γ grains containing stacking faults) along with untransformed α′-martensite and a trace fraction of ε-martensite. In the case of the same steel cold-rolled to 42% thickness reduction and subjected to isochronal annealing, an electron back-scattering diffraction (EBSD) study estimated an activation energy of 237.2 ± 17.3 (kJ/mol) for γ grain growth between 700 and 900 °C annealing; a value that suggests the operation of grain boundary diffusion [19]. In addition, the activation energy of γ grain growth in Fe-29Mn-0.06C high Mn steel during isothermal annealing at 1000 °C was estimated as 208 kJ/mol [20]. In this regard, the activation energy for γ grain growth for Fe-1.51Mn-0.03Si-0.17C, Fe-1.43Mn-0.03Si-0.12C and Fe-0.86Mn-0.03Si-0.11C plain carbon steels is estimated as ~262, 271 and 272 kJ/mol respectively [21]; values that are slightly higher than high Mn steel. For C-Mn-V, C-Mn-Ti, C-Mn-Nb based micro-alloyed low carbon steels, the activation energy for γ grain growth is reported as 400, 437 and 435 kJ/mol respectively [22]; values that are almost double those compared to high Mn steels. Digital image correlation during room temperature, uniaxial tension after cold-rolling and isochronal annealing revealed strain localisation accompanying deformation-induced phase transformation all along the parallel gauge length [13].

In this regard, the present study presents an overview of the effect of isochronal annealing on the microstructure, texture and mechanical properties of a 42% cold-rolled high manganese steel via a combination of EBSD, transmission electron microscopy (TEM) and room temperature uniaxial tensile testing. It details the orientations of deformation-induced ε and α′-martensite that lead to particular γ orientations upon reversion. Furthermore, this is the first study to segment the γ phase into its reverted/recovered and recrystallised fractions in order to catalogue the differences in morphology and micro-texture between them.

2. Experimental and analytical procedure

An Fe-17Mn-3Al-2Si-1Ni-0.06C steel was slab cast and reheated at 1100 °C for 7200 s. The slab was hot-rolled at 1100 °C to 52.5% thickness reduction in 4 passes to 516 (length) × 60 (width) × ~9.8 (thickness) mm^3. The hot-rolled specimens were subsequently cold-rolled to 42% thickness reduction in 11 passes to 759 (length) × 60 (width) × ~5.4 (thickness) mm^3.

Dog-bone shaped ASTM-EM8-04 standard subsize tensile samples of dimensions 35 (gauge length) × 6 (width) × 2 (thickness) mm^3 were wire-cut from the centre of the cold-rolled sheet parallel to the rolling (RD), transverse (TD) and normal (ND) directions, respectively. Similarly, 10 (length, RD) × 7 (width, TD) × ~5.4 (thickness, ND) mm^3 rectangular samples were wire-cut from the centre of the cold-rolled sheet. The dog-bone and rectangular samples were isochronally annealed at 500, 600, 625, 650, 700, 750, 800 and 850 °C for 300 s and immediately water quenched. In this regard, Supplementary Fig. S1 shows the schematic diagram for processing and subsequent sample preparation.

The hardness of the cold-rolled and annealed rectangular samples was measured using a Struers EmcoTest Durascan-70 equipped with a Vickers indenter using a 10 kgf load on the ND-RD plane. Ten indents were undertaken on each sample and the average hardness reported along with the standard deviation. The softening fraction (X) was calculated from the hardness values using the equation [23]:

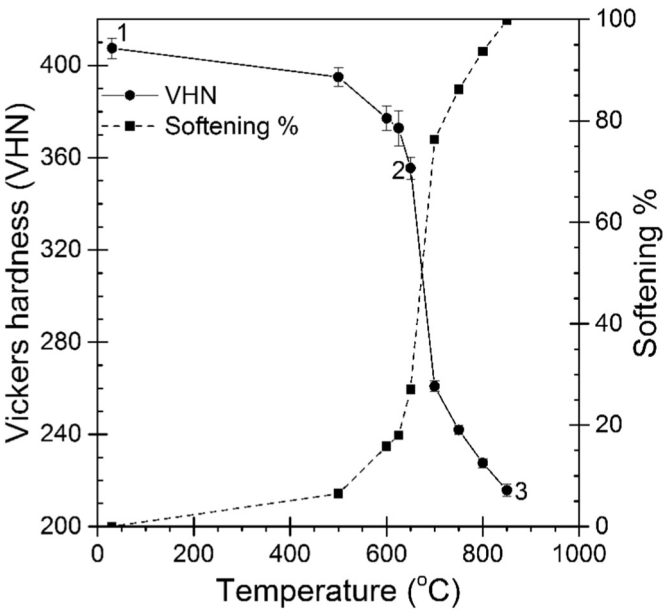

Fig. 1. Variation in hardness and the softened fraction with annealing temperature.

$$X = (H_R - H_T)/(H_R - H_0) \quad (1)$$

where, H_R is the hardness after cold-rolling, H_T is the hardness after annealing at temperature 'T' between 500 and 800 °C and H_0 is the hardness after annealing at 850 °C.

The dog-bone samples were subjected to uniaxial tension at room temperature on a 100 kN Instron1341 universal testing machine operating with an initial crosshead speed of 0.035 mm/s at a strain rate of 0.001 s^{-1}.

Electron transparent thin foils for microstructural characterisation via EBSD and transmission electron microscopy (TEM) were prepared by punching 3 mm diameter discs from the ND-RD plane. The punched discs were ground using 2400 grit abrasive paper to achieve a final thickness of ~60–70 μm and then twin-jet electropolished at −25 °C using a solution of 90% methanol and 10% perchloric acid in a Struers Tenupol-5 operating at 30 V (~150 mA).

For texture characterisation, the RD-ND plane of the rectangular samples was ground using 2400 grit abrasive paper and electro-polished in a Struers LectroPol-5 operating at 50 V for 90 s with a solution of 330 ml methanol, 330 ml butoxyethanol and 40 ml perchloric acid.

EBSD was undertaken on a JEOL JSM-7001F field emission gun-scanning electron microscope operating at 15 kV accelerating voltage, ~6.5 nA probe current. The working distances for electron transparent foils and rectangular samples were 12 and 15 mm, respectively. For microstructure characterisation, a step size of 0.03 μm was used for the cold-rolled, 500, 625 and 650 °C annealed samples. A step size of 0.1 μm was used for the 700–850 °C annealed samples. For bulk texture work, a step sizes of 1 μm was used for the cold-rolled and 500–650 °C annealed samples, 2 μm for the 700 and 750 °C annealed samples and 2.5 μm for the hot-rolled, 800 and 850 °C annealed samples.

Post-processing of the EBSD maps for microstructure characterisation was undertaken using the Oxford Instruments (OI) Channel-5 software suite. In brief, it involved the removal of wild spikes and cyclic extrapolation of zero solutions up to five neighbours followed by thresholding the band contrast to delineate the unindexed regions. The band contrast map was superimposed on the phase maps such that the red, green, blue and white colours denote the γ, ε, α′-martensite phases and unindexed regions, respectively. Boundary misorientations of 2°–15° and greater than 15° comprise low (LAGBs) and high (HAGBs)-angle grain boundaries, respectively. As per the Palumbo-Aust criterion ($\Delta\theta \leq 15^\circ\ \Sigma^{-5/6}$), Σ3 γ-twin boundaries have a maximum angular